



## Halogen bond in separation science: A critical analysis across experimental and theoretical results

Paola Peluso<sup>a,\*</sup>, Victor Mamane<sup>b,\*</sup>, Alessandro Dessì<sup>a</sup>, Roberto Dallochio<sup>a</sup>, Emmanuel Aubert<sup>c</sup>, Carlo Gatti<sup>d</sup>, Debby Mangeling<sup>e</sup>, Sergio Cossu<sup>f</sup>

<sup>a</sup> Istituto di Chimica Biomolecolare ICB, CNR, Sede secondaria di Sassari, Traversa La Crucca 3, Regione Balduca, Li Punti, Sassari I-07100, Italy

<sup>b</sup> Institut de Chimie de Strasbourg, UMR CNRS 7177, Equipe LASYRO, 1 rue Blaise Pascal, Strasbourg Cedex 67008, France

<sup>c</sup> Cristallographie, Résonance Magnétique et Modélisations (CRM2), UMR CNRS 7036, Université de Lorraine, Bd des Aiguillettes, Vandoeuvre-les-Nancy 54506, France

<sup>d</sup> CNR-SCITEC, Istituto di Scienze e Tecnologie Chimiche "Giulio Natta", sezione di via Golgi, via C. Golgi 19, Milano 20133, Italy

<sup>e</sup> Department of Analytical Chemistry, Applied Chemometrics and Molecular Modelling, Vrije Universiteit Brussel – VUB, Laarbeeklaan 103, B-1090 Brussels, Belgium

<sup>f</sup> Dipartimento di Scienze Molecolari e Nanosistemi DSMN, Università Ca' Foscari Venezia, Via Torino 155, Mestre Venezia I-30172, Italy

### ARTICLE INFO

#### Article history:

Received 24 September 2019

Received in revised form 9 December 2019

Accepted 11 December 2019

Available online xxx

#### Keywords

Chromatography

Enantioseparation

Halogen bond

Molecular modelling

Separation science

### ABSTRACT

The halogen bond (XB) is a noncovalent interaction involving a halogen acting as electrophile and a Lewis base. In the last decades XB has found practical application in several fields. Nevertheless, despite the pivotal role of noncovalent interactions in separation science, investigations of XB in this field are still in their infancy, and so far a limited number of studies focusing on solid phase extraction, liquid-liquid microextraction, liquid-phase chromatography, and gas chromatography separation have been published. In addition, in the last few years, our groups have been systematically studying the potentiality of XB for HPLC enantioseparations. On this basis, in the present paper up-to-date results emerging from focused experiments and theoretical analyses performed by our laboratories are integrated with a descriptive presentation of XB features and the few studies published until now in separation science. Then, the aim of this article is to provide a comprehensive and critical discussion of the topic, and account for some still open issues in the application of XB to separate chemical mixtures.

© 2019

### 1. Introduction

Separation science deals with theory, methods and technologies related to separation of chemical compound mixtures [1–3]. A separation process must be able to discriminate molecules in a multicomponent mixture. Therefore, the knowledge of size, shape, and structure of the molecular components of a mixture is a basic requirement to design a tailored separation system. Indeed, properties of the molecules which are involved in the separation process determine separation mechanisms and noncovalent interactions which underlie mixture separation.

When molecules are at work to carry out a specific function in molecular and supramolecular systems, they relate to each other by means of noncovalent interactions [4,5], which represent the essential elements of the code by which molecules are able to transfer the information contained in their structure [6]. These molecular relationships are the basis of mechanisms in several fields [7], and also make noncovalent interactions a modern tool for design, preparation and function of advanced processes and materials in separation science [8].

Among noncovalent interactions, in the last decades halogen bonds (XBs) have found practical applications in several fields covering catalysis, crystal engineering, functional and soft materials, molecular recognition, supramolecular chemistry and biological, medicinal and pharmaceutical chemistry [9–11]. Nevertheless, separation processes promoted by XB are reported in smaller degree [8,12–16]. In particular, despite the pivotal role of noncovalent interactions in LC enantiomer distinction [17,18], surprisingly, for a long time XBs were unexplored in the enantioseparation science [19].

Various reasons have contributed to make the study of XB in separation science challenging. First, halogen substituents can contribute to separation and molecular recognition process by playing multiple roles (hydrophobic site, electron-withdrawing atom, repulsive interaction site, hydrogen bond acceptor), and the presence of electrophilic regions on bound halogens has to be confirmed theoretically. Indeed, XB comprehension mostly depends on its physical description at theoretical level [20–22]. Then, often separation processes occur in solution, and the study of XB in solution [23] is a more demanding task compared to solid state studies. For example, the chromatography environment is a complex solvated system. Finally, limited availability of brominated and iodinated analytes makes the study of halogen effect on separation processes challenging.

\* Corresponding authors.

E-mail addresses: [paola.peluso@cnr.it](mailto:paola.peluso@cnr.it) (P. Peluso); [vmamane@unistra.fr](mailto:vmamane@unistra.fr) (V. Mamane)

In this perspective, the aim of this paper is to provide a critical analysis of the topic. For this purpose, firstly, XB is profiled by describing its main features. Secondly, the few studies on XB applications in separation science reported so far in the literature are discussed. Then, with the aim to explore and clarify some still open issues, we describe herein up-to-date results performed by our laboratories specifically for this purpose and emerging from i) a theoretical re-examination of some literature studies using the density functional theory (DFT) method, and ii) an experimental exploration under supercritical fluid chromatography (SFC) conditions. This multidisciplinary approach is in agreement with recent trends in separation science where theoretical methods are integrating more and more with experiments in order to develop separation systems with high capacity, robustness, and selectivity.

## 2. Experimental

### 2.1. Chemicals

Compounds **39i**, **39s**, and **39v** were synthesized as reported [24]. Pure enantiomers of compounds **39i**, **39s**, and **39v** were obtained by HPLC enantioseparation and their absolute configuration was assigned on the basis of X-ray diffraction or by comparison of theoretical/experimental electronic circular dichroism spectra, as previously described [25].

### 2.2. Chromatography

For analyses under normal phase (NP) elution conditions, a Merck-Hitachi Lachrom Elite gradient HPLC system with photodiode array detection (Tokyo, Japan) and an Agilent Technologies (Waldbronn, Germany) 1100 Series HPLC system (Agilent Technologies ChemStation Version B.04.03 chromatographic data software) were employed. Analyses in SFC were performed using a Waters UPC<sup>2</sup> system with photodiode array detection. Carbon dioxide (CO<sub>2</sub>) with quality 4.5 (purity > 99.995%) was from Messer, (Sint-Pieters-Leeuw, Belgium). Lux Cellulose-1 (Phenomenex, USA) (cellulose *tris*(3,5-dimethylphenylcarbamate); 5 μm), was used as chiral column (250 × 4.6 mm). HPLC grade *n*-hexane, and 2-propanol were purchased from VWR Chemicals (Leuven, Belgium) and Sigma-Aldrich (Taufkirchen, Germany). Analyses were performed in isocratic mode at 22 and 25 °C. The flow rate was set at 0.8 and 1 ml/min. The enantiomer elution order (EEO) was determined for compounds **39i**, **39s**, and **39v** by injecting enantiomers of known absolute configuration.

### 2.3. Computational

Geometry optimization and computation of electrostatic potentials mapped on 0.002 au electron density isosurfaces ( $V_S(\mathbf{r})$ ) and related parameters ( $V_S(\mathbf{r})$  extrema, maxima ( $V_{S,\max}$ ) and minima ( $V_{S,\min}$ ) values, given in kJ/mol or au) were performed and graphically generated by using Spartan' 10 Version 1.1.0 (Wavefunction Inc., Irvine, CA) [26] (DFT method with the B3LYP functional and the 6-311G\* basis set) and Gaussian 09 (Wallingford, CT 06492, USA) [27] (DFT/B3LYP/def2-QZVP and DFT/M06-2X/def2-QZVP [28]). Values of  $V_S(\mathbf{r})$  were used as an indicator of the molecular charge distribution [29]. On the electron density isosurface, colours towards red depict negative mapped potentials, while colours towards blue depict positive potentials and colours in between (orange, yellow, green) depict intermediate values of the mapped potential. Search for the exact location of  $V_{S,\max}$  and  $V_{S,\min}$  was made through the Multiwfn code [30] and through its module enabling quantitative analyses of molecular surfaces [31] for several isovalue surface fields and mapped properties thereon. For compounds **39s**, **39t**, and **39u**, electrostatic potential source func-

tion decomposition analysis was performed through a methodology previously reported [32].

## 3. Halogen bond

### 3.1. Brief history

The first observed XB-based association was the iodine-ammonia complex (I<sub>2</sub>...NH<sub>3</sub>) obtained by Colin in 1814 through the reaction of iodine and gaseous ammonia [33]. Later the same complex was reported by Guthrie upon reaction between iodine and liquid ammonia [34]. Then, other theoretical and experimental studies were performed, nevertheless for a long time these data were unable to provide a comprehensive picture of the XB [9].

On the contrary, in the late twentieth century, important observations and experiments brought the great potential of XB to light, and allowed to recognize that the electrophilic behaviour of halogens is a commonplace event rather than exceptional, occurring in the solid, liquid and gas phase [9,10]. The first use of the term XB can be traced back to the study of Zingaro and Hedges in 1961 [35], the authors describing the complexes formed between halogens and phosphine oxides or phosphine sulphides. In 1968, Bent published a review on the chemistry of donor-acceptor adducts, where he treated about "Organic Molecules with Oxygen Atoms as Electron Donors and Halogen Atoms as Acceptors" and "Molecules with Halogen Atoms as Electron Donors and/or Acceptors". In this paper, the author highlighted the distinctive geometric features of the interactions, evidencing that the distances between the electron donor atom and the halogen atom were shorter than the sum of their respective van der Waals radii [36]. Later, in his Nobel lecture, Hassel considered that "Particular importance may be attributed to complexes in which direct bonding exists between one atom belonging to the donor molecule and another atom belonging to the acceptor molecule. Complexes of this kind are above all those formed by donor molecules containing atoms possessing "lone pair electrons" and halogen or halide molecules" [37].

Finally, in 2013 the International Union of Pure and Applied Chemistry issued the "Definition of the halogen bond (IUPAC recommendations 2013)" stating that "a halogen bond occurs when there is evidence of a net attractive interaction between an electrophilic region associated with a halogen atom in a molecular entity and a nucleophilic region in another, or the same, molecular entity" [38].

### 3.2. Halogen bond and $\sigma$ -hole bonds

In 1992, Brinck, Murray and Politzer proposed the first theoretical explanation of the XB introducing two basic concepts: the anisotropic charge distribution on bound halogens and the definition of the  $\sigma$ -hole as a region of electronic charge density depletion, which is located on the surface of halogen atoms and usually characterized by a positive electrostatic potential [39]. On this basis, the XB originates from the anisotropic charge distribution which characterizes bound halogens, in particular when they are bound to electron-withdrawing groups (EWGs). It means that an area of lower electron density, located on the elongation of the covalent bond, the  $\sigma$ -hole, coexists with an area of higher electron density, which forms a belt orthogonal to the covalent bond (Fig. 1) [40].

Other atoms were found to interact by means of  $\sigma$ -hole regions, therefore XBs are a subset of the so-called  $\sigma$ -hole bonds. This wide family of noncovalent interactions involves the electrophilic region of electronic charge density depletion, the  $\sigma$ -hole, centred on bound atoms of groups 13–18 ( $\sigma$ -hole donors), which behave as Lewis acids, and a  $\sigma$ -hole acceptor, a Lewis base (Table 1) [41].

3.3. Features of the halogen bond  
The anisotropic charge distribution explains the amphoteric behaviour of the halogens which behave as Lewis bases, or as XB donors

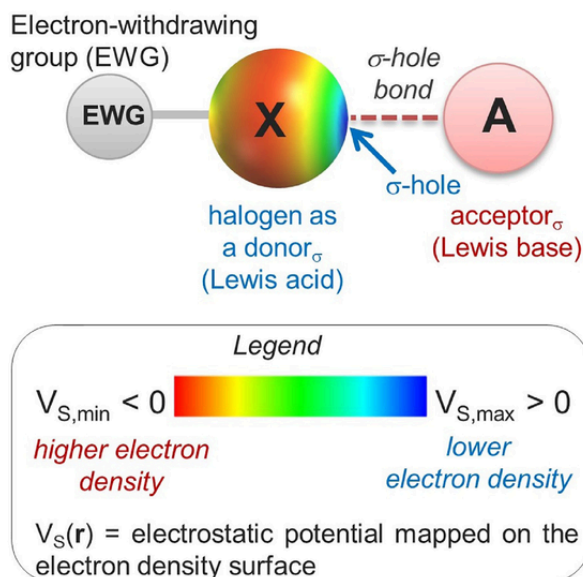
Fig. 1. General description of  $\sigma$ -hole and halogen bond.

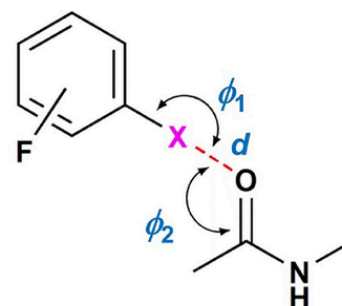
Table 1  
Noncovalent interactions based on electrophilic  $\sigma$ -holes.

$\sigma$ -hole bond		
$\sigma$ -hole donor (Lewis acid)	-----	$\sigma$ -hole acceptor (Lewis base)
Donor <sub>σ</sub> (Lewis acid)	$\sigma$ -holebond	Acceptor <sub>σ</sub> (Lewis base)
B, Al, Ga, In, Tl (group 13)	Triel bond	O, N, S, halogen, $\pi$ -donor, anion
C, Si, Ge, Sn (group 14)	Tetrel bond	
P, As, Sb, Bi (group 15)	Pnictogen bond	
S, Se, Te (group 16)	Chalcogen bond	
F, Cl, Br, I (group 17)	Halogen bond	
Kr, Xe (group 18)	Aerogen bond	

with properties of Lewis acids able to interact with an acceptor through the  $\sigma$ -hole. The most important feature of the XBs is tunability, the strength of a XB depending on the properties of donor, acceptor and medium, and it increases as the polarizability and the electronegativity of the halogen increases and decreases, respectively. So, XB strength increases following the order  $F < Cl < Br < I$ , bromine and iodine being considered as more powerful XB donors. Concerning medium, in general solvents possessing hydrogen bond donor functionalities destabilize the XBs because of XB-hydrogen bond competition. Indeed, molecules with properties as Lewis bases can act as acceptors towards both halogen and hydrogen bond donors.

Another distinctive feature of the XB is directionality (Fig. 2), with defined geometrical parameters, angles and distance (typical values for I...O contacts:  $2.8 \text{ \AA} \leq d_{I...O} \leq 3.4 \text{ \AA}$ , sum of I, O vdW radii being  $3.5 \text{ \AA}$  [42]). In this regard, a parameter to measure the strength of the XB is the penetration parameter (*p.p.*) [24,43] which is calculated as the percentual reduction of the sum of van der Waals radii of the interacting atoms, indicating the penetration degree of the van der Waals spheres.

Due to the physical nature of the XBs, computational tools and studies *in silico* have greatly contributed to their understanding [20], explaining experimental results and guiding experiment design. In particular,  $\sigma$ -hole being a region of electronic charge density depletion, calculated  $V_S(\mathbf{r})$  has been widely used as an indicator of the anisotropy



## GEOMETRICAL PARAMETERS

$\phi_1$  C—X—O angle (reference value  $180^\circ$ )

$\phi_2$  X—O=C angle (reference value  $120^\circ$ )

$d_{X...O}$  (A) typical distances 80-98% sum of van der Waals radii

## PENETRATION PARAMETER % =

$$100 \times \{(d_{X...A}) / (r_{vdW} X + r_{vdW} A) - 1\}$$

where X = halogen, A = acceptor,  
 $d_{X...A}$  = interatomic distance,  
and  $r_{vdW}$  is the van der Waals radius

Fig. 2. Geometrical parameters of the halogen bond.

of the molecular charge distribution. In this regard, the evaluation of the  $V_{S,\max}$  on the halogen surfaces allows for a quantitative estimation of the  $\sigma$ -hole depth [44] which, in turn, determines the capability of a halogen as XB donor.

Nowadays the nature of XB still remains matter of hot discussion in order to define the relative importance of electrostatic, dispersion, charge transfer and polarization contributions when XB occurs [9,45,46]. In this regard, it is worth noting that the studies on the nature of the XB, which have been published so far, tend to be often contradictory in their conclusions. It is likely that this apparent lack of coherence is due to the fact that the relative importance of the different contributions depends on the system, which consists of donor, acceptor and medium [10].

On the other hand, the general features of the XB are well explained on the basis of its electrostatic nature. In particular, a pure electrostatic model gives reasonable correlations to experimental data gathered in apolar solvents, even if it is unsuitable for the description of XBs in polar systems [23].

Recently, Clark proposed a protocol consisting of three levels of interaction for the analysis of weak intermolecular interactions such as XB [47]: (i) a first level containing the classical  $\delta^+ - \delta^-$  electrostatic interactions (*permanent electrostatic interactions*) that can be evidenced by inspecting the unperturbed  $V_S(\mathbf{r})$  at the standard isodensity surfaces of an isolated molecule [29], (ii) the second level improves the previous view by introducing the mutual polarization of interacting molecules (*induced electrostatic interactions*), and (iii) finally, the third level includes dispersion, which is not a real, measurable quantity and can only be observed as a difference between mean-field calculations and those that consider electron correlation.

## 4. Halogen bond in separation science: a literature survey

### 4.1. Solid-phase extraction of iodoperfluoroalkanes

In 2012, Jin and co-workers described the unprecedented utilization of XB in the solid phase extraction of perfluorinated iodoalkanes

(PFIs) from *n*-hexane. A strong anion-exchange (SAX) sorbent (1) (Fig. 3) functioning as XB acceptor was used, which forms an associate with PFIs 2 and 3 behaving as XB donors [12]. PFIs are persistent organic pollutants, being key intermediates for the synthesis of fluorochemicals and fluoropolymers. In this study, following a multidisciplinary approach,

nine PFIs, as test probes, were analysed by UV,  $^{19}\text{F}$  NMR and Raman spectroscopies in order to demonstrate the occurrence of C-I...Cl $^-$  XB interactions. The results showed that the adsorptivities of SAX for the  $\alpha,\omega$ -diiodoperfluoroalkanes (DIPFAs) 2 were stronger than those for the monoiodo-PFIs 3. In particular, SAX proved to have no adsorption for hexafluorobenzene, which has no properties as XB donor.

Therefore, the application of XB in solid-phase extraction provides a new retention mechanism in extraction processes. Moreover, this investigation paved the way to the utilization of XB in chromatography and to the idea, which our group will develop later (§ 5), that XBs could also work on chiral sorbents to promote enantiomer distinction.

It is worth mentioning that in 2009 Resnati and co-workers had shown that the organic salts bis(trimethylammonium)alkane diiodides 4 (Fig. 4) could resolve mixtures of DIPFAs 2 by means of crystallization from solution [48] promoted by I...I $^-$  XB interactions. Interestingly, the solid-state salts could also selectively bind the DIPFAs from the vapour phase, yielding the same adducts formed from solution.

Later, the group of Jin also investigated the adsorption of iodoperfluoroarenes (IPFAs) (Fig. 5) on SAX promoted by XB, using again *n*-hexane as a solvent [49]. On the basis of  $^{19}\text{F}$  NMR titration experiments, UV spectrometric titrations and theoretical calculations, the authors showed that Cl $^-$ , as the XB acceptor, is better than Br $^-$  and I $^-$ . The adsorption efficiency of IPFAs on SAX followed the order 1,4-DITFB (5)  $\approx$  1,2-DITFB (6) > IPFB (7), with no significant adsorption of bromoperfluoroarenes. Interestingly, prominent red shifts of characteristic Raman spectra showed that XB is unambiguously the main driving force of the adsorption process.

#### 4.2. Molecularly imprinted polymers

In 2005, a molecularly imprinted polymer (8) (Fig. 6) bearing XB-based binding sites was developed by Takeuchi and co-workers for application in separation science [16]. The formation of this imprinted polymer host was obtained by the polymerization of the functional monomer 2,3,5,6-tetrafluoro-4-iodostyrene (9), as the XB donor, with divinylbenzene and styrene as cross-linking agents, in the presence of 4-(dimethylamino)pyridine (10) as the XB acceptor templating guest.

Indeed, the authors had envisaged that the XB acceptor template could recognize the XB donor sites on the host polymer, imprinting the molecular shape of the guest into the polymer (8) and generating spe-

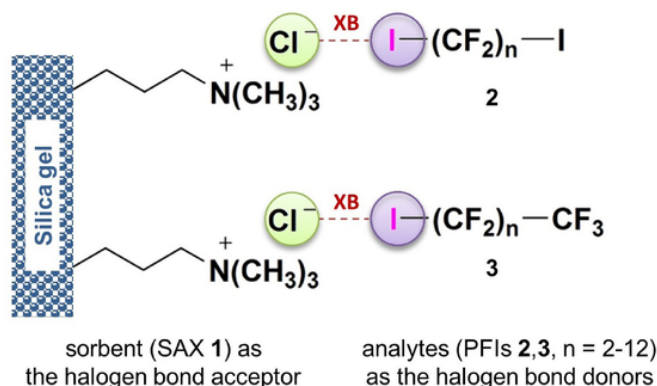


Fig. 3. Interaction models of the PFIs (2,3) and Cl $^-$  on the SAX sorbent (1).

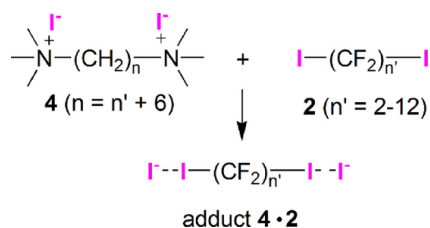


Fig. 4. XB adduct between bis(trimethylammonium)alkane diiodides (4) and DIPFAs (2).

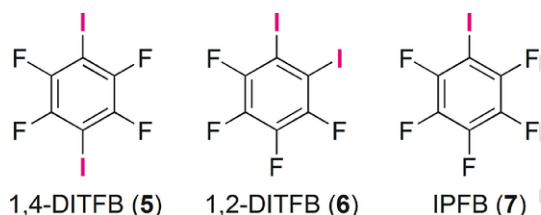


Fig. 5. Structures of IPFB, 1,2- and 1,4-DITFB.

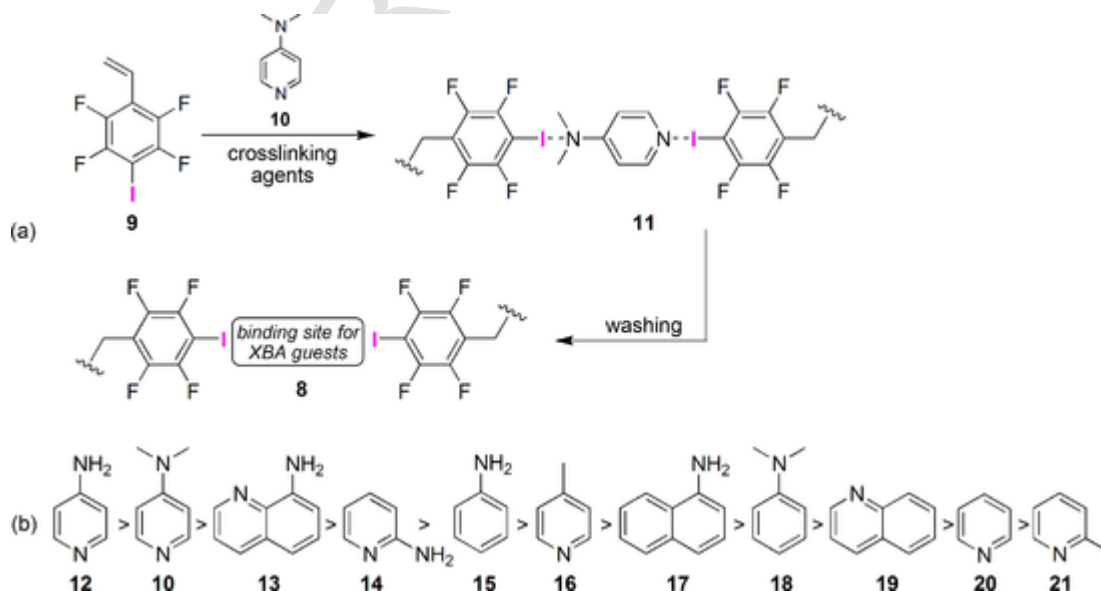


Fig. 6. (a) Preparation scheme of the molecularly imprinted polymer developed using 4-(dimethylamino)pyridine as XB acceptor template; (b) affinity order of the XB acceptor guests.



cific binding sites selective for **10** and its structural analogues. On this basis, the binding affinity of the imprinted polymer was investigated by using XB acceptors **10** and **12–21** bearing either aliphatic or aromatic nitrogen groups. As expected, the 4-aminopyridine guests **12** and **10** showed the highest affinities for the porous polymer, which exhibited a high affinity for the less bulky 4-aminopyridine (**12**), suggesting that nitrogen basicity and steric hindrance may influence the recognition mechanism.

#### 4.3. Halogen bond in liquid-liquid microextraction

Recently, Sicilia and co-workers proposed a solubilisation mechanism based on XB and dispersion interactions for increasing the efficiency in the liquid-liquid microextraction of hexabromocyclododecane (HBCD) stereoisomers (**22**) (Fig. 7) in river water, by using a supramolecular solvent (SUPRAS) (**23**), which is made up of inverted hexagonal aggregates of decanoic acid in tetrahydrofuran and water [13,50]. HBCDs are brominated flame retardants used in industry that can be released into the environment. For SUPRAS **23**, two types of interactions with **22** were hypothesized: XB through the oxygen atom of the carboxylic acid and dispersion interactions in the hydrocarbon chains.

The same XB-based microextraction procedure had been previously proposed by the same group for speeding up the extraction of HBCD in soils and sediments [51] and fish [52]. Unfortunately, these studies suffer from the fact that the proposed mechanism was not supported by spectroscopic analyses or theoretical calculations on both donor (HBCD) and acceptor (SUPRAS).

#### 4.4. Halogen bond in gas chromatography separation of haloarenes

The utilization of XB can open new possibilities for GC separation of halocarbons, a class of industrially relevant compounds. In particular, chlorobenzenes **24** and polychlorobiphenyls (PCBs) **25** (Fig. 8a) are key molecules for chemical industries and environmental analysis.

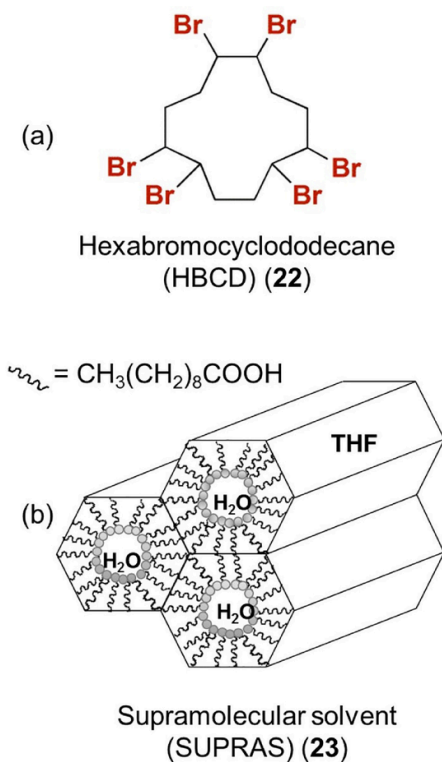


Fig. 7. (a) Structure of HBCD; (b) scheme of the nanostructure of SUPRAS.

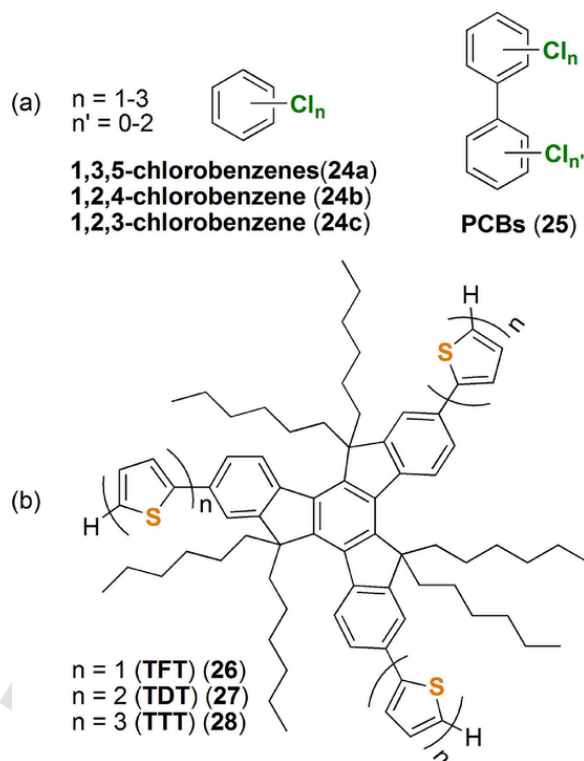


Fig. 8. (a) analytes separated on truxene-based stationary phases; (b) chemical structure of TFT, TDT and TTT.

In the last few years, Qi, Wang and co-workers developed thio-phenyl-functionalized truxene derivatives (TFT **26**, TDT **27**, TTT **28**) [14,53] as new types of stationary phases for GC separations (Fig. 8b). The separation ability of these supports towards **24** and **25** was explored. A longer retention was observed for **24c**, which was attributed by the authors to a strong XB between the chlorines of the analyte (XB donors) and the sulfur atoms (XB acceptors) of side chains of **26**. Moreover, hypothesizing again a XB-based retention mechanisms, the authors performed the separation of three trichlorobenzene isomers of **24** on **28** with the retention order  $24a < 24b < 24c$ .

Later, the same group reported the development of a propeller-like hexaphenylbenzene-based hydrocarbon material (BT) (**29**) (Fig. 9a) [54] which was used as the stationary phase for capillary GC. The BT capillary column showed weak polarity and interesting selectivity for aromatic compounds, the stationary phase being characterized by  $\pi$ -electron toroidal delocalization and intrinsic microporosity. In particular, the trichlorobenzene isomers **24** were well resolved, the authors hypothesizing combined interactions of XB ( $\text{Cl}\cdots\pi$ ) (Fig. 9b),  $\pi$ - $\pi$  stacking and van der Waals.

Very recently, Qi, Huang and co-workers published a series of papers dealing with the development of triptycene (TP)-based materials **30–33** for capillary GC separations (Fig. 10) [15,55,56]. These stationary phases exhibited high-resolution performances for a wide range of analytes, especially halogenated structural and positional isomers. In particular, the fact that the stationary phase **30** retained bromohexane longer than cyclohexanone was explained by means of a XB involving the bromine substituent of the analyte. The same explanation was used to justify the elution sequence nitrobenzene (**34**)  $<$  1,3,5-trichlorobenzene (**24a**) and naphthalene (**35**)  $<$  m-dibromobenzene (**36**), which appeared to be against the order of boiling points of the analytes.

Qi, Cai and co-workers reported the first example of pillar[n]arenes **37** used as a new type of stationary phase for GC separations [57]. Pillar[n]arenes are a class of macrocycle hosts made up of hydroquinone units linked by methylene bridges at the 2,5-positions, with a

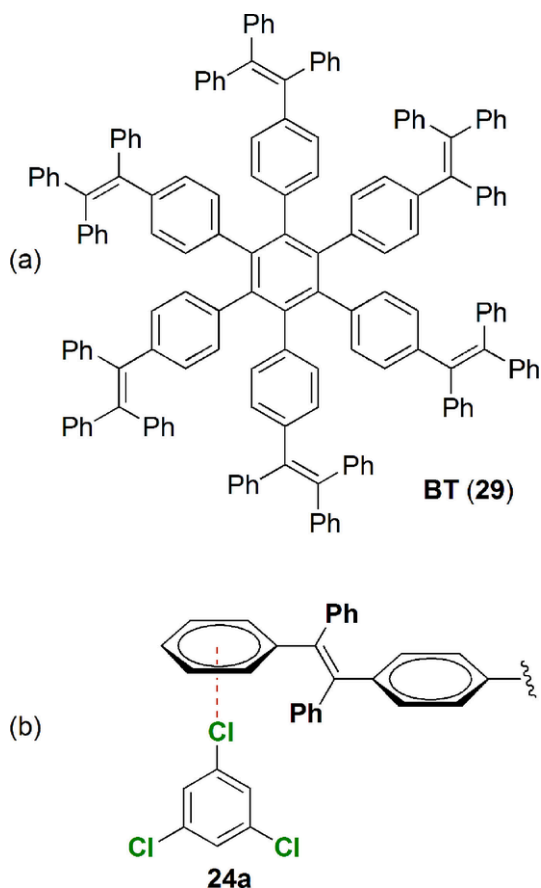


Fig. 9. (a) Chemical structure of propeller-like hexaphenylbenzene-based stationary phase (BT); (b) halogen bond interaction (C... $\pi$ ) of terminal residue of the stationary phase with 1,3,5-trichlorobenzene 24a.

highly symmetrical and rigid pillar architecture and an electron-rich cavity. Also in this case, the retention behaviour and the high-resolution performance towards dibromoalkanes **38** was attributed to the possibility that XB can function in this GC environment.

Finally, recently, our group also explored the possibility of XB-based GC separation [58], and retention and selectivity of polyhalogenated 4,4'-bipyridines (HBipys) **39a-r** were evaluated on Hydrodex- $\beta$ -PM (heptakis-(2,3,6-tri-O-methyl)- $\beta$ -cyclodextrin) and Chirasil Val (N-propionyl-L-valine-tert-butylamide polysiloxane) capillary columns, both containing oxygen sites as potential XB acceptors. Despite the fact that no obvious trend related to the identity of the XB emerged from the chromatographic data, the presence of iodine substituents seemed to increase retention on both columns. Moreover, the three compounds **39i**,

**39o**, and **39q**, which were enantioseparated on Hydrodex- $\beta$ -PM, contained iodines.

It is worth noting that all XB-based mechanisms proposed until now in GC separation represent working hypotheses which were not supported by focused spectroscopic studies, calculations or analysis in the solid state. Moreover, in these studies the separation of iodinated benzenes is missing, consequently the effect of halogens on separation of halobenzenes was only partially evaluated.

With the aim to tackle this unexplored question by means of a case study, we calculated  $V_{S,max}$ ,  $V_{S,min}$ , and related surface parameters for HBipys **39a-r** (Table 2) and the presence of structure-GC chromatographic behaviour relationships were verified by linear regression analysis. The results reported in Table 3 show a strong correlation between retention times and molecular weight (MW), area and enclosed volume of calculated electrostatic potential surfaces, revealing a leading mechanism controlled by the analyte shapes. On the other hand, two minor statistically significant correlations were derived between retention time on both columns and  $V_{S,max}$  values on the halogens ( $r^2 = 0.4961$ ;  $0.4837$ , P-value =  $0.0011$ ;  $0.0014$ ) and  $V_{S,min}$  on the nitrogen ( $r^2 = 0.4151$ ;  $0.4075$ , P-value =  $0.0039$ ;  $0.0044$ ), revealing a possible minor contribution of both XB and hydrogen bond to retention.

#### 4.5. Halogen bond in normal phase liquid chromatography

Very recently, Kubo and co-workers experimentally evaluated the strength of the X... $\pi$  interaction between carbon-materials and a series of halogenated benzenes under NP elution conditions [8], assuming that the hydrophobic interaction was completely suppressed in this environment. Under these conditions, higher retentions were observed as the number of Cl, Br, or I substituents on the benzenes increased, especially for the C70-coated column **40** (Fig. 11), which showed higher retention efficiency than other carbon materials. In particular retention of hexahalobenzenes increased in the order  $F < Cl < Br < I$ . The carbon-materials are known to exhibit strong  $\pi$  interactions because of their numerous  $\pi$  electrons. By using a multidisciplinary approach based on the combined use of chromatographic analysis, UV-Vis and NMR spectroscopy, and computational calculations, the authors envisaged the existence of bimodal interactions, the  $\pi$ - $\pi$  and X... $\pi$  interactions, between the halogenated benzenes and aromatic materials.

#### 5. Halogen bond in enantioseparation science

So far, XB in chiral systems has been reported in small degree, and few chiral XB donors and enantioselective processes promoted by XBs are known [9].

The first example in enantioseparation science dates back to 1999, when Metrangolo and Resnati used the Lewis base (-)-sparteine hydrobromide (**41**) (Fig. 12) to resolve the racemic 1,2-dibromohexafluoropropane (**42**) [59]. The resolution occurred as a result of a highly spe-

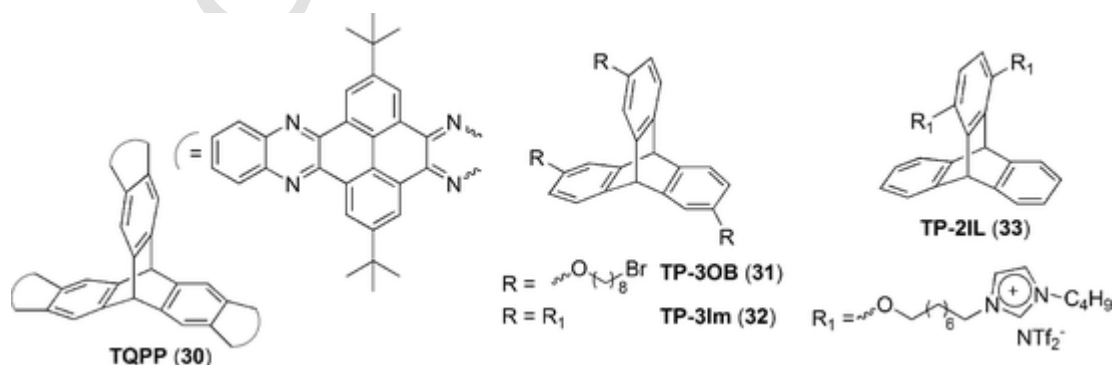
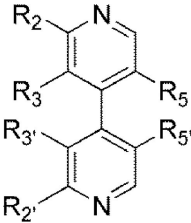


Fig. 10. Structure of TP-base materials used as stationary phase for GC separations, TQPP, TP-2IL, TP-3OB, and TP-3Im.

**Table 2**  
Retention times on Hydrodex- $\beta$ -PM and Chirasil-Val chiral capillary columns [58], and calculated molecular properties<sup>a</sup> of HBipys **39a-r**.  
Expand



**39a-r**

HBipy 39	Substitution pattern R <sub>2</sub> -R <sub>2</sub> '-R <sub>3</sub> - R <sub>3</sub> '-R <sub>5</sub> -R <sub>5</sub> '	MW	V <sub>S,max</sub> (X) [kJ/ mol]	V <sub>S,min</sub> (N) [kJ/ mol]	surface area [Å <sup>2</sup> ]	surface volume [Å <sup>3</sup> ]	Hydrodex- $\beta$ -PM t <sub>1</sub> (t <sub>2</sub> ) [min]	Chirasil-Val-t <sub>1,2</sub> [min]
a	H-H-I-H-Cl-Cl	350.97	134.4	-156.9	237.9	240.4	8.82	7.60
b	H-H-I-H-Br-Br	439.87	131.6	-158.2	246.8	251.8	12.08	10.54
c	H-H-I-I-Cl-Cl	476.87	136.9	-140.4	262.3	274.6	13.43	11.79
d	H-H-I-I-Br-H	486.87	131.6	-158.0	253.1	262.5	15.26	13.14
e	H-H-I-I-Br-Br	565.77	134.1	-141.5	270.1	286.2	19.93	17.07
f	Cl-Cl-Br-Br-Br-Br	540.66	123.3	-131.1	285.3	299.7	24.78	20.08
g	Cl-Cl-I-H-Br-Br	508.76	151.3	-142.9	278.2	287.1	25.27	20.03
h	Cl-Cl-Cl-Cl-I-I	545.76	154.4	-128.7	292.5	309.5	29.66	23.70
i	Cl-Cl-I-I-Cl-Cl	545.76	154.3	-130.6	289.7	309.0	32.05 (32.65)	25.64
j	Cl-Cl-I-I-Br-I	555.76	151.3	-142.9	285.4	297.7	34.92	27.14
k	Cl-Cl-Br-Br-Br-I	587.66	153.3	-131.4	292.2	310.3	35.33	28.02
l	Br-Br-I-H-Br-Br	597.66	149.7	-143.6	288.1	298.5	43.53	35.02
m	Cl-Cl-I-H-I-I	602.76	151.8	-144.1	291.9	308.3	47.09	38.78
n	Cl-Cl-Br-Br-I-I	634.66	151.7	-131.6	298.7	320.6	48.10	40.35
o	Cl-Cl-I-I-Br-Br	634.66	151.7	-132.6	297.3	320.4	49.05 (49.70)	42.35
p	Br-Br-Cl-Cl-I-I	634.66	152.3	-130.3	302.4	320.8	50.27	43.32
q	Br-Br-I-I-Cl-Cl	634.66	150.8	-131.6	299.5	320.3	53.30 (54.10)	47.17
r	Br-Br-Br-Br-Br-I	676.56	149.5	-133.1	301.7	321.5	57.89	35.48

<sup>a</sup> Computation of electrostatic potential surfaces and related parameters were performed and graphically generated using the Spartan'10 Version 1.1.0 (Wavefunction Inc., Irvine, CA) program and employing the density functional theory (DFT) method with the B3LYP functional and the 6-311G<sup>a</sup> basis set.

**Table 3**  
Linear regression analysis<sup>a</sup> describing the relationships between retention on Hydrodex- $\beta$ -PM and Chirasil-Val chiral capillary columns [58] and calculated molecular properties of HBipys **39a-r**.

Independent variable	Hydrodex- $\beta$ -PM		Chirasil-Val	
	r <sup>2</sup>	P-value	r <sup>2</sup>	P-value
MW	0.8595	0.0000	0.8052	0.0000
surface <sub>ED</sub> area <sup>b</sup>	0.8183	0.0000	0.7828	0.0000
surface <sub>ED</sub> volume <sup>b</sup>	0.8021	0.0000	0.7772	0.0000
V <sub>S,max</sub> (X)	0.4961	0.0011	0.4837	0.0014
V <sub>S,min</sub> (N)	0.4151	0.0039	0.4075	0.0044

<sup>a</sup> Statgraphics Centurion XVI (Statpoint Technologies, Inc., Warrenton, VA, USA) was used for all linear regression analyses.

<sup>b</sup> Surface<sub>ED</sub>, electron density surface.

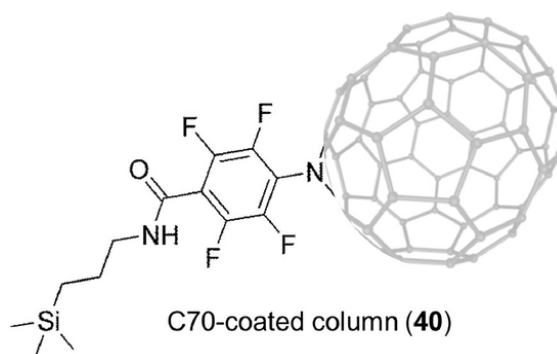


Fig. 11. Structure of the C-70 coated column **40**.

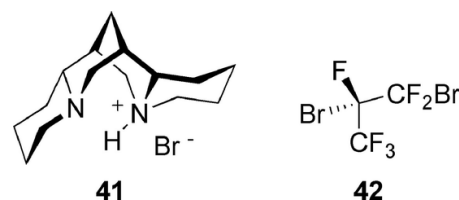


Fig. 12. Structure of the XB acceptor **41** and XB donor **42**.

cific inclusion of only the (*S*)-enantiomer in a chiral crystal with a helical arrangement formed by XB between the C-bound Br atoms of **42** and the Br<sup>-</sup> ions of **41**. Later, the same group performed the resolution of racemic perfluorocarbons by means of a XB-driven electron donor-acceptor recognition mechanism [60].

In the field of enantioseparation science, HPLC on chiral stationary phase is widely used. In this environment, the distinction process is based on the ability of the chiral selector to recognize the enantiomers by means of stereoselective noncovalent interactions, which are strictly dependent on chiral selector, analyte and mobile phase.

In 1996, Pirkle and co-workers had highlighted an unexpected halogen effect on the HPLC enantioseparation of halogenated amide derivatives of 1-phenylethylamine [61]. Nevertheless, in this study,

where Pirkle considered that “Unexpectedly, para and meta halogen substituents increase both retention and enantioselectivity when nonaqueous organic mobile phases are used. The more polarizable the halogen, the greater the effect”, halogen-dependent effects on enantioselectivity were never explicitly related to the XB. The reason was likely due to the fact that for a long time F, Cl, Br and I substituents in LC enantioselectivity were merely considered as a Lewis base, in the perspective of an isotropic distribution of the electron density [62]. On this basis, it can be expected that XB-driven enantioselectivities could be recognized by means of a theoretical re-examination of some published enantioselectivity processes.

### 5.1. Enantioselectivities involving XB on polysaccharide-based CSPs: a multidisciplinary approach integrating theoretical analysis with experiments

Starting from 2014, XBs being still unexplored in HPLC enantioselectivity, our group envisaged that HPLC, as a technical tool, could be successfully used to systematically investigate XBs occurring on the surface of the chiral adsorbent by properly tuning molecular properties of analyte as XB donor, selector as XB acceptor, under NP elution conditions [22,25,58]. With this purpose, cellulose dimethylphenylcarbamate (CDMPC) **43** was selected as chiral stationary phase (CSP) (Fig. 13a) because of a negative  $V_{S,\min}$  ( $-173.3$  kJ/mol) which makes carbonyl functionality a good halogen  $\sigma$ -hole acceptor, similar in terms of  $V_{S,\min}$  and site structure to other typical acceptors like acetone ( $-177.0$  kJ/mol) or *N*-methylacetamide ( $-216.3$  kJ/mol). As analytes, we have developed halogenated donors based on the electron

poor 4,4'-bipyridine core (**39a-v**) (Fig. 13b) [24], where halogens serve as  $\sigma$ -hole sites, and inductors of chirality by restricted rotation around the 4,4'-bipyridyl bond. The enantioselectivity of functionalized 4,4'-bipyridines being dependent on the substituents carried by the heteroaromatic scaffold [19], the chromatographic response of the halogenated analogues is strictly dependent on the  $\sigma$ -hole depth, XB strength increasing from chlorine to bromine and iodine. Some halogenated bipyridines were studied in the solid state [24,25], and nitrogen-halogen contacts, with penetration parameters increasing from chlorine to iodine ( $-15.1$  (N...I)  $\leq p.p. \leq -2.8$  (N...Cl)), were observed, these results proving the capability of these halogens to act as  $\sigma$ -hole donors.

To tackle the study of XB in HPLC environment, the use of distinct orthogonal techniques provides complementary information for a more comprehensive picture of XB-based enantioselectivity processes which are the result of a balanced synergy between CSP, analyte, and mobile phase. Therefore, in the last few years we have approached the question by means of a multidisciplinary study involving chromatographic analysis, X-ray diffraction analysis and theoretical calculations [22,24,58].

### 5.2. Computational tools to design XB donors as test probes and to rationalize related recognition mechanisms

The quantitative assessment of  $V_{S,\max}$  and  $V_{S,\min}$  have been found to be related to the strengths of noncovalent interactions [20,29]. In particular, the depth of  $\sigma$ -hole on halogens is related to their XB donor capability. In this regard, Murray and co-workers highlighted the importance of identifying methods and basis sets that are reliable for computing properly  $V_{S,\max}$  and  $V_{S,\min}$  [29]. In general, too large basis sets are not needed for this purpose. Indeed, electrostatic potential values are computed for the unperturbed molecules prior to interaction in order to assess what they are likely to do. On this basis, with the aim to demonstrate the concept, herein, the  $V_{S,\max}$  values of three representative compounds **39s-u** are reported comparing different functionals and basis sets (Table 4). The  $\sigma$ -hole on halogens increases as the atomic number of the halogen with all theoretical methods, even with the smaller basis set (DFT/B3LYP/6-311G\*), which gives slightly more positive  $V_{S,\max}$  and generates larger variations in  $\sigma$ -hole magnitude [20,29]. Indeed, M06-2X and def2-QZVP variations of  $V_{S,\max}$  on the halogen  $\sigma$ -hole are smaller.

According with calculated  $V_{S,\max}$  on halogens, the enantioselectivity of compounds **39a-v** on the CSP **43** under NP elution conditions increased following the order Cl < Br < I, and  $V_{S,\max}$  on iodine substituents, ranging from 149 kJ/mol to 154 kJ/mol, were found on compounds enantioselectively separated with high selectivity values ( $\alpha > 2.00$ ) [58].

Correlating molecular properties and experimental results allows for a better understanding of mechanisms underlying the discrimination process. Taking into account the hydrophobic character of halogenated compounds, two competitive mechanisms are envisaged to contribute to retention and selectivity. The unreported case study described in Fig. 14 has been designed and performed with the aim to prove the concept. CDMPC and *n*-hexane/2-propanol 9:1 (flow rate 0.8 ml/min,  $T = 22$  °C) were used as CSP and mobile phase, respectively. Under these elution conditions, the two *P* enantiomers of compounds **39i** and **39v** are eluted with very similar retention times and free energy changes associated with the complex formation. This means that the retention of the *P* enantiomers is governed by forces which are highly similar in the two enantiomers and related to their molecular shape, thus revealing a mechanism controlled by the steric fit of the *P* stereoisomers into the polymer groove. Differently, the *M* enantiomers show different elution times and free energy changes which can be reasonably related to the different  $\sigma$ -hole depth around the chiral axis. Consequently, the EEO reversal from *P,M* for **39i** to *M,P* for **39v**, is re-

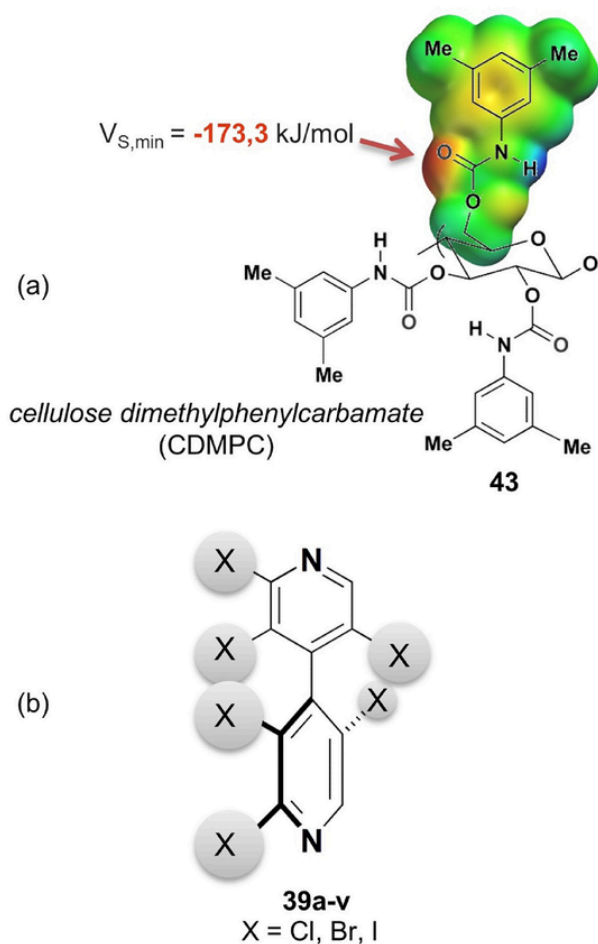



Fig. 13. Chromatographic system developed for the study of XB in HPLC environment: (a) CDMPC polymer as the CSP; (b) polyhalogenated 4,4'-bipyridines as the analytes.



**Table 4**  
 $V_{S,max}$  on halogen  $\sigma$ -holes for compounds 39s-u.  
 Expand



program/calculation level	$V_{S,max}$ [kJ/mol] <sup>a</sup>				
	CH <sub>3</sub> Cl	39s (X = Cl)	39t (X = Br)	39u (X = I)	iodopentafluorobenzene
Spartan <sup>b</sup> /DFT/B3LYP/6-311G*	5.9	89.9 (1.00)	119.8 (1.333)	144.2 (1.604)	164.6
Gaussian <sup>c</sup> /DFT/B3LYP/def2-QZVP	-	75.7 (1.00)	93.7 (1.238)	114.2 (1.509)	-
Gaussian <sup>c</sup> /DFT/M06-2X/def2-QZVP	-	77.9 (1.00)	93.2 (1.200)	116.1 (1.490)	-

<sup>a</sup> In parentheses are given the relative values of the brominated and iodinated analogues normalized with respect to the chlorinated bipyridine 39s.

<sup>b</sup> Spartan '10 Version 1.1.0 (Wavefunction Inc., Irvine, CA).

<sup>c</sup> Gaussian 09 (Wallingford, CT 06492, USA).

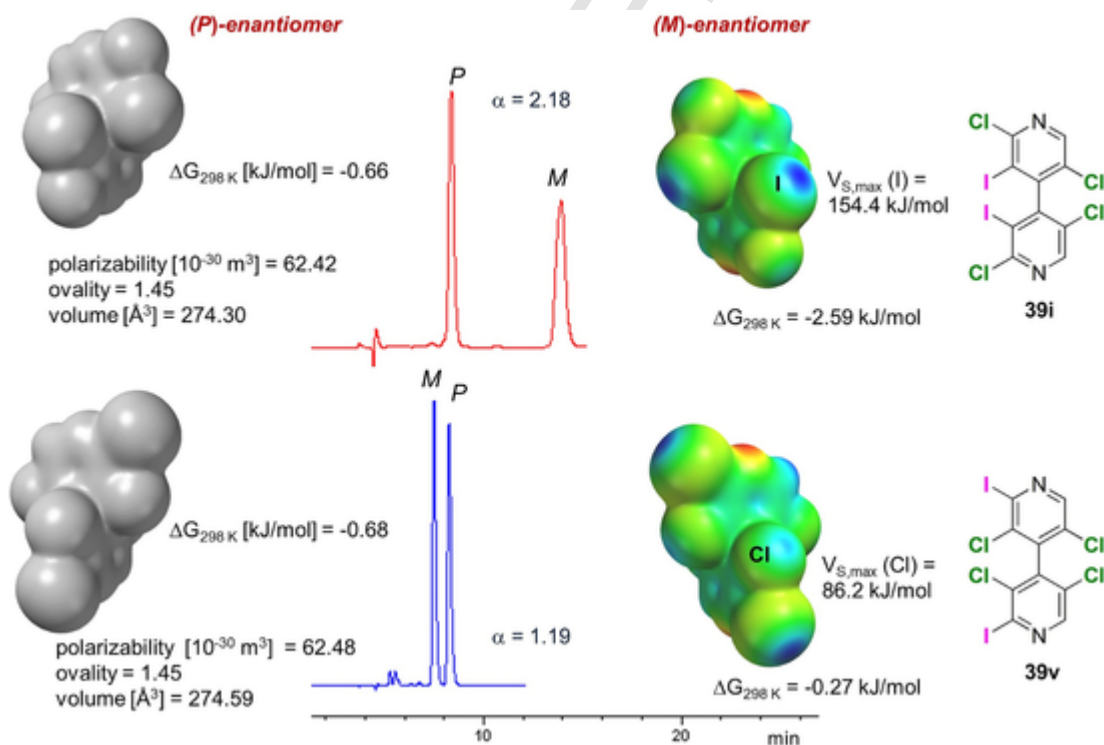


Fig. 14. Comparison of enantiorecognition mechanisms of compounds 39i and 39v (CDMPC, *n*-hexane/2-propanol 9:1, flow rate 0.8 ml/min,  $T = 22$  °C).

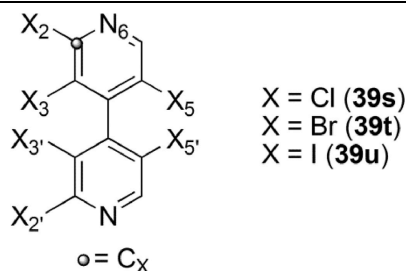
lated to the fact that, for 39i, the iodine bond-driven mechanism is more efficient, in terms of enantiomer-CSP complex stability, compared to the mechanism based on the steric fit. On the contrary, for compound 39v, the chlorine bond-driven mechanism is less efficient, so the *M* stereoisomer becomes the first eluted.

To examine in depth the origin of the observed  $V_{S,max}$ , within a cause-effect view, we calculated the contribution of each atom of the molecule to generate the positive  $V_{S,max}$  on the halogen (X)  $\sigma$ -holes

by means of the source function mathematical tool [63], on the basis of a theoretical methodology applied by our group to the reconstruction of chalcogen  $V_{S,max}$  [32]. In Table 5, the results of the electrostatic potential source function decomposition applied to the X-centred  $\sigma$ -holes in compounds 39s-u are summarized. The sign of source function is positive or negative whether the atomic source concurs or opposes to the positive potential of  $\sigma$ -hole. This feature allows us to identify the molecular frameworks which contribute to the electrophilic charac-

**Table 5**  
Electrostatic potential source function (SF) decomposition of  $V_{S,max}$  at the X-centred  $\sigma$ -holes in compounds **39s-u**.

Expand



Expand	2	3	4	5	6	7	8	9
X(position)	SF%(own ring)	SF%(other ring)	SF(X)	SF(C <sub>X</sub> + X)	SF(N <sub>6</sub> )	SF(N <sub>6</sub> + C <sub>X</sub> + X)	SF [own ring –(N <sub>6</sub> + C <sub>X</sub> + X)]	$V_{S,max}$ $\sigma$ -hole[au] <sup>a</sup>
I (2)	95.3	4.7	0.071	0.109	-0.119	-0.010	0.059	0.0507
Br (2)	93.5	6.6	0.034	0.102	-0.128	-0.026	0.063	0.0403
Cl (2)	90.1	10.9	-0.006	0.093	-0.133	-0.041	0.067	0.0286
I (3)	98.7	1.9	0.081	0.048	-0.091	-0.043	0.102	0.0599
Br (3)	96.0	4.8	0.040	0.034	-0.097	-0.063	0.111	0.0498
Cl (3)	90.6	10.0	-0.003	0.018	-0.100	-0.082	0.118	0.0386
I (5)	99.1	1.6	0.076	0.039	-0.093	-0.054	0.114	0.0606
Br (5)	96.5	4.2	0.033	0.023	-0.098	-0.075	0.124	0.0501
Cl (5)	90.9	9.1	-0.010	0.006	-0.102	-0.096	0.131	0.0387

<sup>a</sup> Computation of electrostatic potential surfaces were performed and graphically generated using the Spartan'10 Version 1.1.0 (Wavefunction Inc., Irvine, CA) program and employing the density functional theory (DFT) method with the B3LYP functional and the 6-311G\* basis set. Search for the exact location of  $V_{S,max}$  was made through the Multiwfn code [30] and through its module enabling quantitative analyses of molecular surfaces [31].

ter of halogens, furnishing valuable information to design properly compounds with properties as XB donors. Considering as reference points the  $\sigma$ -holes centred on X ( $n$ ) ( $n = 2, 3, 5$ ), the contribution of the pyridine ring bearing X ( $n$ ) is dominant (column 2) compared to the contribution of the other ring (column 3). This response was expected on the basis of the atropisomeric topology of the two orthogonal aryl planes. Moreover, the values reported in Table 5 show that the trend  $V_{S,max}$  (I) >  $V_{S,max}$  (Br) >  $V_{S,max}$  (Cl) for the  $\sigma$ -holes (column 9) originates from a corresponding trend of the X (column 4), (C<sub>X</sub> + X) (column 5), and N<sub>6</sub> (column 6) contributions which is only partly compensated for by an opposite trend in the remaining ring sources (column 8). These observations highlight the pivotal role that the substituents exert on the stereoelectronic properties of the electrophilic recognition sites, guiding properly analyte design. Moreover, the different halogen contribution to the  $\sigma$ -holes of **39s** (negative) with respect to **39u** (positive) could fully justify the difference in HPLC selectivity of the two compounds ( $\alpha$ : 1.16 (**39s**), 2.68 (**39u**) [25]), enantioseparation being driven by XBs on the cellulose-based CSP **43** under NP elution conditions.

Finally, it is worth mentioning that, for the study of XB in HPLC environment, molecular dynamics simulations [22,64] are extremely versatile to reproduce the experimental chromatographic system account-

ing for solvent effect and mutual conformational adjustment of analyte and selector, and to predict EEO. In particular, good agreement between experimental and simulated data was achieved by using the explicit  $\sigma$ -hole (ESH) tool [20,21] in order to account for the electrophilic character of the halogen moieties.

### 5.3. HPLC enantioseparations involving XB donors as analytes: a theoretical re-examination

In HPLC, the enantioseparations of fluorinated and chlorinated compounds are more frequent compared to those of brominated or iodinated compounds. In particular, very recently the XB has been proposed as a noncovalent interaction involved in the enantioseparation of some chlorinated compounds (Fig. 15) on polysaccharide-based CSPs. Okino and co-workers hypothesized that the enantioseparation of Columbamide D (**44**) on Chiralpak AD-H is possibly driven by a XB between chlorine on the analyte and the carbamate carbonyl group of the stationary phase [65]. On the basis of docking results, Wang and co-workers proposed the occurrence of a XB between the chlorine atom on the benzene ring of Cyproconazole (**45**) and an oxygen atom on the Lux Cellulose-2 CSP [66]. Link and co-workers proposed, on the basis

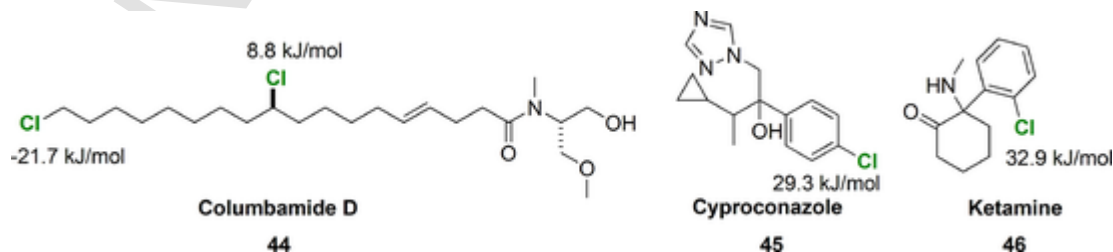


Fig. 15.  $V_{S,max}$  on chlorine  $\sigma$ -hole in Columbamide D, Ketamine, and Cyproconazole.

of docking data, the possibility of XB between the chlorine substituent of Ketamine (**46**) as an analyte and the carbonyl group of the *i*-Amylose-3 CSP [67].

In this regard, with the aim to evaluate the  $\sigma$ -hole depth on chlorines in **44–46**, we calculated the  $V_{S,max}$  on chlorines at DFT level of theory (B3LYP/6-311G\*) and the results are reported in Fig. 15. Positive  $V_{S,max}$  values ranging from 8.8 to 32.9 kJ/mol were found, the  $V_{S,max}$  on the primary chlorine of Columbamide D being negative (–21.7 kJ/mol). On this basis, limited involvement is expected for the three compounds **44–46** as XB donors in the HPLC environment, chlorines being characterized by calculated  $V_{S,max}$  on  $\sigma$ -holes lower than 50 kJ/mol [58], and functioning in competitive systems, where hydrogen bond centres are also present as recognition sites [22].

The question of the possibility of fluorine to be involved in XB in LC enantioselectivity remains rather undefined [68]. Indeed, fluorine is less prone to behave as XB donor due to its high electronegativity and low polarizability, and it can act as an electrophile only when attached to strong EWGs like –CN or –F [9].

### 5.5. Exploiting halogen bond in enantioseparation science: open issues and perspectives

In the next subsections, we describe a series of new results emerging from experiments and theoretical calculations specifically designed and performed in order to assess open issues perspectives of XB utilization in (enantio)separation science.

#### 5.5.1. Halogen bonds in supercritical fluid chromatography enantioseparations: possible role of CO<sub>2</sub>

Non-polar pressurized carbon dioxide is considered a hexane-like solvent with respect to its elution strength [69]. Therefore, the replacement of *n*-hexane to carbon dioxide should cause no important changes in retention and selectivity [70]. In reality, carbon dioxide is not hexane-like because it is more polarizable, and it has local dipoles (C=O bonds) and partial charges on both carbon and oxygen [70]. Theoretical calculations and related experimental data proved that carbon dioxide can form XB-based (O=C=O...X) associations where it acts as XB acceptor [71]. In this perspective, with the aim to verify the chromatographic response of halogenated chiral analytes under SFC conditions, we compared retention and selectivity of the enantiomeric pairs of compounds **39i** and **39s**, used as test probes, under SFC (carbon dioxide/2-propanol 9:1) and NPLC (*n*-hexane/2-propanol 9:1) on CDMPC (Fig. 13a) (column: Lux Cellulose-1) in order to explore the effect of changing *n*-hexane to carbon dioxide on retention and enantioselectivity. Under NPLC conditions, **39i** is enantioseparated with good selectivity ( $\alpha = 2.30$ , EEO = *P,M*) through a recognition mechanism based on I...O contacts, as stereoselective secondary interactions, iodine being a good XBD [58]. On the contrary, the selectivity value decreased in the case of **39s** ( $\alpha = 1.22$ , EEO = *M,P*), chlorine being a poor XB donor [58]. The results of the SFC/NPLC comparative experiments are presented in Table 6. In both cases, the flow rate was 1 mL/min.

For both racemates **39i** and **39s**, SFC conditions displayed lower elutropic power than NPLC conditions, retention factors being from three to seven times higher in SFC than in HPLC, with retention increment higher for **39i** compared to **39s**. Indeed, for compound **39i**, NPLC condition produced baseline resolution within 12 min, whereas SFC conditions yielded a longer 49 min analysis, at the same  $T = 25^\circ\text{C}$ . Differently, analysis time increase was not so pronounced for compound **39s** (elution time: NPLC, 5 min; SFC, 9 min). On this basis, polyhalogenated analytes as XB donors show stronger retention in SFC. Taking into account that on the CDMPC the carbonyls are acceptors for both XB donors and hydrogen bond donors, our results are consistent with the fact that the interaction ability of CDMPC toward hydro-

**Table 6**

Enantioseparation of HBipys **39i** and **39s** on CDMPC ( $FR = 1\text{ mL/min}$ ,  $T = 25^\circ\text{C}$ ) under NP (*n*-hexane/2-propanol 9:1) and SFC (carbon dioxide/2-propanol 9:1) conditions. <sup>a, b</sup>

HBipy	MP <sup>c</sup>	k <sub>1</sub>	k <sub>2</sub>	$\alpha$
<b>39i</b>	NP	1.40 (1.00)	3.22 (1.00)	2.30 (1.00)
	SFC	9.82 (7.01)	14.61 (4.54)	1.49 (0.65)
<b>39s</b>	NP	0.49 (1.00)	0.60 (1.00)	1.22 (1.00)
	SFC	1.74 (3.55)	1.88 (3.13)	1.08 (0.89)

<sup>a</sup> Column: Lux Cellulose-1 (Phenomenex, 5 $\mu$ ) (CDMPC), 250  $\times$  4.6 mm. Detection wavelength, 220 nm.

<sup>b</sup> In parentheses are given the relative values of SFC chromatographic parameters normalized with respect to NPLC parameters.

<sup>c</sup> MP, mobile phase.

gen bond donors was reported to be stronger in SFC with respect to NPLC [70].

Both enantiomer pairs **39i** and **39s** were eluted in SFC keeping unchanged NPLC EEO. However, a decrease of selectivity for both analytes (**39i**, –35%; **39s**, –11%) was observed in SFC compared to NPLC, due to a different effect of carbon dioxide on the retention of the second eluted enantiomers compared to the first eluted. Indeed, for the two second eluted enantiomers, the retention increase, moving from NPLC to SFC conditions, is lower (4.54 and 3.13 times longer for **39i** and **39s**, respectively) than the retention increase of the first eluted enantiomers (7.01 and 3.55 times longer for **39i** and **39s**, respectively). In particular, for **39i**, the effect is higher resulting in a higher decrease of selectivity compared to **39s**.

At the molecular level, the same effect on both enantiomers could be expected if the CO<sub>2</sub> acts as *n*-hexane (non-interacting solvent). On the contrary, according with the experimental data, a different effect of CO<sub>2</sub> is foreseeable if it associates with halogens, reasonably forming XB-based solvation clusters. In this context, halogens are less prone to be involved in XB with the CSP, thus the presence of CO<sub>2</sub> is more detrimental for **39i** which forms stronger XBs.

On this basis, further investigations are needed to confirm these preliminary observations on the potential role of carbon dioxide in XB-based SFC recognition processes, a question so far unexplored.

#### 5.5.2. Potential function of halogenated polysaccharide-based CSPs as XB donors: a theoretical examination

Polysaccharide carbamates-based CSPs are the most used for HPLC enantioseparations [72]. The polysaccharide backbone is the essential element of this polymeric system, with the conformational chirality depending on the peculiar helical twist generated by specific glycosidic linkages in cellulose and amylose polymeric chains [72–74]. Significantly, the polymer backbone is functionalized with a polar layer containing carbamate moieties able to exert polar interactions and located inside the polymer groove, and a hydrophobic layer containing substituted aromatic rings, located outside the polymer groove and able to activate  $\pi$ - $\pi$  interactions (Fig. 13a) with analytes. Nowadays, different types of polysaccharide-based CSPs are commercially available, and the side chains are characterized by distinctive steric and electronic properties which are the key to the different selectivity of the corresponding CSPs. Indeed, the electronic properties of the polar layer and its ability to exert hydrogen bonds are tuned by changing type and position of both alkyl- and chloro substituents onto the terminal aromatic ring [72,74]. On the other hand, studies on fluorinated, brominated and iodinated CSPs were published [75,76] in the late twentieth century.

Until recently, no systematic study has been performed about the possible electrophilic behaviour of the chlorine located on polysaccharide-based CSPs. However, some authors speculated that XB could underlie recognition mechanisms on chlorinated CSPs. In this regard, West and co-workers stated “Halogen bonds should also be considered

as possible contributors to the specific retention and separation behavior of chlorinated CSP" [77], and later Jiang and co-workers considered "the halogen bonding occurred as an intermolecular interaction when chlorine atom acted as an electron density acceptor (Lewis acid) and tended to interact with electron donor partners. In this regard, the chlorine atom on CSP phenyl can interact with the C=O group and phenyl ring of the enantiomer by halogen-carbonyl oxygen and halogen- $\pi$  interactions, respectively. Based on the above reasons, both the electron-withdrawing inductive effect and the halogen bonding produced by chlorine atoms of CSP appeared to be favorable for the enantioseparation" [78].

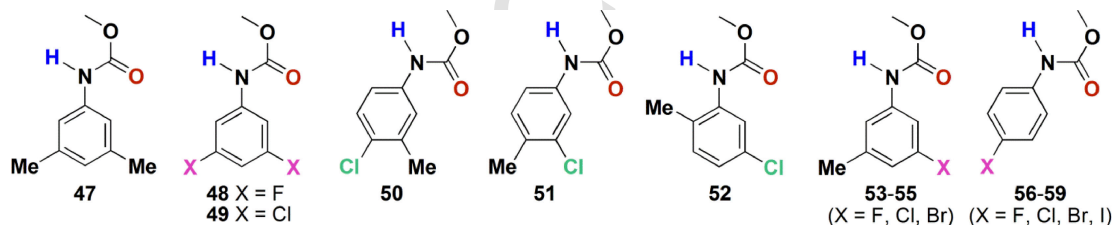
We report herein a theoretical examination of the electronic properties of some halogenated side chains associated with commercially available CSPs (Table 7, side chains 47, 49–52, 54, 57) or reported in the literature with respect to their preparation and enantioseparation performances (side chains 48, 53, 55, 56, 58, 59). For each side chain, we calculated (DFT/B3LYP/6-311G\*) the  $V_{S,max}$  and  $V_{S,min}$  on carbamate N-H and C=O, respectively, as indicators of their capability as hydrogen bond donor and acceptor. In addition, the  $V_{S,max}$  on halogen  $\sigma$ -holes were considered in order to get a quantitative estimation of the capability of the halogens as electrophilic XB donors.

The following observations emerged:

1) as expected, fluorine, as substituent of the phenylcarbamates, does not present a  $\sigma$ -hole with positive  $V_{S,max}$  and negative values of  $V_{S,max}$  ranging from  $-81.5$  kJ/mol to  $-61.4$  kJ/mol were calculated for side chains 48, 53 and 56. Therefore, in principle, for the corresponding CSPs, XB cannot underlie retention and enantioselectivity;

- 2) in the case of chlorine, positive  $V_{S,max}$  values ranging from 12.0 kJ/mol to 41.4 kJ/mol revealed the presence of electrophilic  $\sigma$ -holes on halogens, but small in magnitude. On this basis, the potential of these chlorines to be involved in XB is rather limited, in particular considering that the corresponding N-H — moieties (side chains 49–52, 54 and 57), are competitive sites, showing higher positive  $V_{S,max}$  ( $209.5$  kJ/mol  $\leq V_{S,max} \leq 249.5$  kJ/mol). Therefore, it is likely that analytes with properties as XB and hydrogen bond acceptors show a preference towards N-H—, which is more electrophilic as recognition site;
- 3) higher positive  $V_{S,max}$  were calculated for bromine in side chains 55 and 58, and as expected, the highest  $V_{S,max}$  value was found for iodine in the side chain 59;
- 4) from a re-examination of some chromatographic results reported by Okamoto and co-workers [75], an interesting trend was observed in the comparative retention of four chiral compounds containing XB acceptors as recognition sites, namely *trans*-stilbene oxide (60), Tröger base (61), flavanone (62) and 2-phenylcyclohexanone (63) (Fig. 16), on the cellulose-based CSPs containing 4-halophenyl side chains 56–59. Indeed, for this series of analytes, the retention factors of the first eluted enantiomers increase as the  $V_{S,min}$  on the nucleophilic recognition sites ( $60 < 61 < 62 < 63$ ) only with the iodinated 59-containing CSP, whereas a different trend ( $60 < 61 < 63 < 62$ ) was observed on the other three cellulose-based CSPs. Moreover, it is worth noting an EEO reversal for 62 by changing 56–58-containing CSPs (enantiomer (+)) to the iodinated 59-containing CSP (enantiomer (-)).

**Table 7**  
Calculated  $V_{S,max}$  and  $V_{S,min}$  [kJ/mol] on carbamate N—H and C=O, respectively, and  $V_{S,max}$  [kJ/mol] on halogen (X)  $\sigma$ -holes of substituted phenylcarbamate side chain 47–59.  
Expand



side chain(Ar substituents)	$V_{S,max}$ N-H	$V_{S,min}$ C=O	$V_{S,max}$ X( $\sigma$ -hole)	side chain(Ar substituents)	$V_{S,max}$ N-H	$V_{S,min}$ C=O	$V_{S,max}$ X( $\sigma$ -hole)
47 (3,5-diMe)	206.8	-173.3	-	54 (3-Cl,5-Me)	228.6	-155.9	26.9 (Cl)
48 (3,5-diF)	243.2	-151.9	-68.7 (F)	55 (3-Br,5-Me)	229.2	-156.4	61.9 (Br)
49 (3,5-diCl)	249.5	-147.3	41.4 (Cl)	56 (4-F)	228.5	-161.5	-81.5 (F)
50 (4-Cl,3-Me)	231.6	-156.5	20.0 (Cl)	57 (4-Cl)	235.3	-155.5	22.7 (Cl)
51 (3-Cl,4-Me)	227.9	-159.2	27.7 (Cl)	58 (4-Br)	235.5	-155.7	57.5 (Br)
52 (5-Cl,2-Me)	209.5	-162.3	12.0 (Cl)	59 (4-I)	236.3	-154.9	87.8 (I)
53 (3-F,5-Me)	225.9	-159.8	-77.4 (F)				

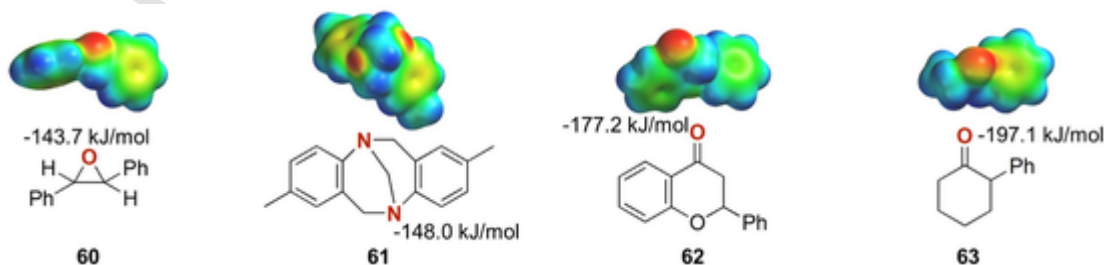


**Fig. 16.**  $V_{S,min}$  on O or N as nucleophilic recognition sites in compounds 60–63.



Two pieces of information emerge from this theoretical examination: a) the presence of halogen in CSP structures does not mean that XB underlies enantiomer distinction and the magnitude of the  $\sigma$ -hole should be always evaluated theoretically; b) the potential function of iodine as XB donor (electrophile) on polysaccharide-based CSPs deserves to be considered in the next future.

## 6. Conclusions and perspectives

The studies published so far have shown that XBs can promote separation processes, where halogens behave as electrophilic descriptors. This aspect is of particular relevance in pharmaceutical, environmental and industrial analyses where the separation of halogenated compounds is not unusual. Nevertheless, the study of XB in separation science is still in its infancy and further investigations are needed in order to find new evidences and make the concept familiar also in this field. For this purpose, a balanced synergy between experimental, theoretical methods and techniques is the best tool to set up appropriate hypotheses and achieve reliable conclusions.

In particular, a growing number of highly directional bromine and iodine-oxygen contacts have been evidenced in biological, medicinal and pharmaceutical chemistry, proving the potential of halogen substituents to contribute to ligand binding through XB [11]. On this basis, in the next future an increasing interest towards compounds containing electrophilic halogen  $\sigma$ -holes is expected in drug discovery and pharmaceutical chemistry. In this perspective, XB as a noncovalent interaction represents a pivotal tool for separation and enantioseparation of pharmaceuticals containing electrophilic holes as recognition sites. Interestingly, the discovery of the first halogen bond-driven self-disproportionation of enantiomers has been recently reported [79].

On the other hand, other interactions involving electrophilic  $\sigma$ -holes could function in separation science. In this regard, recent experiments and calculations have also paved the way for the application of chalcogen and  $\pi$ -hole bonds in separation science [32,80].

## Acknowledgements

This work has been partially supported by Università Ca' Foscari Venezia, Italy (Dipartimento di Scienze Molecolari e Nanosistemi DSMN, ADIR funds). P.P. sincerely thanks Prof. Bezhan Chankvetadze (Tbilisi State University, Georgia) for valuable and stimulating discussions.

## References

- [1] M.T. Bowser, D.D.Y. Chen, Recent developments towards a unified theory for separation science, *Electrophoresis* 19 (1998) 1586–1589.
- [2] G. Guiochon, L.A. Beaver, Separation science is the key to successful biopharmaceuticals, *J. Chromatogr. A* 1218 (2011) 8836–8858.
- [3] N.L. Kuehnbaum, P. Britz-McKibbin, New advances in separations for metabolomics: resolving chemical diversity in a post-genomic era, *Chem. Rev.* 113 (2013) 2437–2468.
- [4] H.J. Schneider, Binding mechanisms in supramolecular complexes, *Angew. Chem. Int. Ed.* 48 (2009) 3924–3977.
- [5] H.J. Schneider, Quantification of noncovalent interactions - Promises and problems, *New J. Chem.* 43 (2019) 15498–15512.
- [6] J.M. Lehn, Supramolecular chemistry - Scope and perspectives, molecules, supermolecules, and molecular devices, *Angew. Chem. Int. Ed.* 27 (1988) 89–112.
- [7] A.S. Mahadevi, G.N. Sastry, Cooperativity in noncovalent interactions, *Chem. Rev.* 116 (2016) 2775–2825.
- [8] E. Kanao, T. Morinaga, T. Kubo, T. Naito, T. Matsumoto, T. Sano, H. Maki, M. Yan, K. Otsuka, Separation of halogenated benzenes enabled by investigation of halogen- $\pi$  interactions with carbon materials, *Chem. Sci.* (2020) DOI: 10.1039/c9sc04906a.
- [9] G. Cavallo, P. Metrangolo, R. Milani, T. Pilati, A. Priimagi, G. Resnati, G. Terraneo, The halogen bond, *Chem. Rev.* 116 (2016) 2478–2601.
- [10] P.J. Costa, The halogen bond: nature and applications, *Phys. Sci. Rev.* (2017) 20170136.
- [11] R. Wilcken, M.O. Zimmermann, A. Lange, A.C. Joerger, F.M. Boeckler, Principles and applications of halogen bonding in medicinal, chemistry and chemical biology, *J. Med. Chem.* 56 (2013) 1363–1388.

- [12] X.Q. Yan, Q.J. Shen, X.R. Zhao, H.Y. Gao, X. Pang, W.J. Jin, Halogen bonding: a new retention mechanism for the solid phase extraction of perfluorinated iodoalkanes, *Anal. Chim. Acta* 753 (2012) 48–56.
- [13] A.B. Lara, C. Caballo, M.D. Sicilia, S. Rubio, Halogen bonding for increasing efficiency in liquid-liquid microextraction: application to the extraction of hexa-bromocyclododecane enantiomers in river water, *J. Chromatogr. A* 1600 (2019) 95–104.
- [14] Q. Zhang, M. Qi, J. Wang, Star-shaped oligothiophene-functionalized truxene materials as stationary phases for capillary gas chromatography, *J. Chromatogr. A* 1525 (2017) 152–160.
- [15] L. Yu, J. He, M. Qi, X. Huang, Amphiphilic triptycene-based stationary phase for high-resolution gas chromatographic separation, *J. Chromatogr. A* 1599 (2019) 239–246.
- [16] T. Takeuchi, Y. Minato, M. Takase, H. Shimori, Molecularly imprinted polymers with halogen bonding-based molecular recognition sites, *Tetrahedron Lett.* 46 (2005) 9025–9027.
- [17] M. Lämmerhofer, Chiral recognition by enantioselective liquid chromatography: mechanisms and modern chiral stationary phases, *J. Chromatogr. A* 1217 (2010) 814–856.
- [18] G.K.E. Scriba, Chiral recognition in separation sciences. Part I: polysaccharide and cyclodextrin selectors, *Trends Anal. Chem.* 120 (2019) 115639.
- [19] P. Peluso, V. Mamane, E. Aubert, S. Cossu, Insights into the impact of shape and electronic properties on the enantioseparation of polyhalogenated 4,4'-bipyridines on polysaccharide-type selectors. Evidence of stereoselective halogen bonding interactions, *J. Chromatogr. A* 1345 (2014) 182–192.
- [20] M.H. Kolář, P. Hobza, Computer modeling of halogen bonds and other  $\sigma$ -hole interactions, *Chem. Rev.* 116 (2016) 5155–5187.
- [21] R. Nunes, D. Vila-Viçosa, P.J. Costa, Tackling halogenated species with PBSA: effect of emulating the  $\sigma$ -hole, *J. Chem. Theory Comput.* 15 (2019) 4241–4251.
- [22] R. Dallochio, A. Dessì, M. Solinas, A. Arras, S. Cossu, E. Aubert, V. Mamane, P. Peluso, Halogen bond in high-performance liquid chromatography enantioseparations: description, features and modelling, *J. Chromatogr. A* 1563 (2018) 71–81.
- [23] A.C.C. Carlsson, A.X. Veiga, M. Erdélyi, Halogen bonding in solution, *Top. Curr. Chem.* 359 (2015) 49–76.
- [24] V. Mamane, P. Peluso, E. Aubert, S. Cossu, P. Pale, Chiral hexalogenated 4,4'-bipyridines, *J. Org. Chem.* 81 (2016) 4576–4587.
- [25] P. Peluso, V. Mamane, R. Dallochio, A. Dessì, R. Villano, D. Sanna, E. Aubert, P. Pale, S. Cossu, Polysaccharide-based chiral stationary phases as halogen bond acceptors: a novel strategy for detection of stereoselective  $\sigma$ -hole bonds in solution, *J. Sep. Sci.* 41 (2018) 1247–1256.
- [26] Y. Shao, L.F. Molnar, Y. Jung, J. Kussmann, C. Ochsenfeld, S.T. Brown, A.T.B. Gilbert, L.V. Slipchenko, S.V. Levchenko, D.P. O'Neil, R.A. Di Stasio Jr, R.C. Lochan, T. Wang, G.J.O. Beran, N.A. Besley, J.M. Herbert, C.Y. Lin, T. Van Voorhis, S.H. Chien, A. Sodt, R.P. Steele, V.A. Rassolov, P.E. Maslen, P.P. Korambath, R.D. Adamson, B. Austin, J. Baker, E.F.C. Byrd, H. Dachsel, R.J. Doerksen, A. Dreuw, B.D. Dunietz, A.D. Dutoi, T.R. Furlani, S.R. Gwaltney, A. Heyden, S. Hirata, C.-P. Hsu, G. Kedziora, R.Z. Khalliulin, P. Klunzinger, A.M. Lee, M.S. Lee, W.Z. Liang, I. Lotan, N. Nair, B. Peters, E.I. Proynov, P.A. Pieniazek, Y.M. Rhee, J. Ritchie, E. Rosta, C.D. Sherrill, A.C. Simmonett, J.E. Subotnik, H.L. Woodcock III, W. Zhang, A.T. Bell, A.K. Chakraborty, D.M. Chipman, F.J. Keil, A. Warshel, W.J. Hehre, H.F. Schaefer, J. Kong, A.I. Krylov, P.M.W. Gill, M. Head-Gordon, Advances in methods and algorithms in a modern quantum chemistry program package, *Phys. Chem. Chem. Phys.* 8 (2006) 3172–3191.
- [27] M.J. Frisch, G.W. Trucks, H.B. Schlegel, G.E. Scuseria, M.A. Robb, J.R. Cheeseman, G. Scalmani, V. Barone, B. Mennucci, G.A. Petersson, H. Nakatsuji, M. Caricato, X. Hratchian, H.P. Li, A.F. Izmaylov, J. Bloino, G. Zheng, J.L. Sonnenberg, M. Hada, M. Ehara, K. Toyota, R. Fukuda, J. Hasegawa, M. Ishida, T. Nakajima, Y. Honda, O. Kitao, H. Nakai, T. Vreven, J.A. Montgomery Jr, J.E. Peralta, F. Ogliaro, M. Bearpark, J.J. Heyd, E. Brothers, K.N. Kudin, V.N. Staroverov, T. Keith, R. Kobayashi, J. Normand, K. Raghavachari, A. Rendell, J.C. Burant, S.S. Iyengar, J. Tomasi, M. Cossi, N. Rega, J.M. Millam, M. Klene, Inc. Gaussian, C.T. Wallingford, Gaussian 09, Revision B. 01 (2010).
- [28] B.P. Pritchard, D. Altarawy, B. Didier, T.D. Gibson, T.L. Windus, A new basis set exchange: an open, up-to-date resource for the molecular sciences community, *J. Chem. Inf. Model.* 59 (2019) 4814–4820.
- [29] K.E. Riley, K.-A. Tran, P. Lane, J.S. Murray, P. Politzer, Comparative analysis of electrostatic potential maxima and minima on molecular surfaces, as determined by three methods and a variety of basis sets, *J. Comput. Sci.* 17 (2016) 273–284.
- [30] T. Lu, F. Chen, Multiwfn: a multifunctional wavefunction analyzer, *J. Comp. Chem.* 33 (2012) 580–592.
- [31] T. Lu, F. Chen, Quantitative analysis of molecular surface based on improved marching tetrahedra algorithm, *J. Mol. Graph. Model.* 38 (2012) 314–323.
- [32] P. Peluso, C. Gatti, A. Dessì, R. Dallochio, R. Weiss, E. Aubert, P. Pale, S. Cossu, V. Mamane, Enantioseparation of fluorinated 3-arylthio-4,4'-bipyridines: insights into chalcogen and  $\pi$ -hole bonds in high-performance liquid chromatography, *J. Chromatogr. A* 1567 (2018) 119–129.
- [33] M. Colin, Note sur quelques combinaisons de l'iode, *Ann. Chim.* 91 (1814) 252–272.
- [34] F. Guthrie, On the iodide of iodammonium, *J. Chem. Soc.* 16 (1863) 239–244.
- [35] R.A. Zingaro, M. Hedges, Phosgene oxide-halogen complexes: effect on P-O and P-S stretching frequencies, *J. Phys. Chem.* 65 (1961) 1132–1138.
- [36] H. Bent, Structural chemistry of donor-acceptor interactions, *Chem. Rev.* 68 (1968) 587–648.
- [37] O. Hassel, Structural aspects of interatomic charge-transfer bonding, *Science* 170 (1970) 497–502.

- [38] G.R. Desiraju, P. Shing Ho, L. Kloo, A.C. Legon, R. Marquardt, P. Metrangolo, P. Politzer, G. Resnati, K. Rissanen, Definition of the halogen bond (IUPAC recommendations 2013), *Pure Appl. Chem.* 85 (2013) 1711–1713.
- [39] T. Brinck, J.S. Murray, P. Politzer, Surface electrostatic potentials of halogenated methanes as indicators of directional intermolecular interactions, *Int. J. Quantum Chem* 44 (1992) 57–64.
- [40] T. Clark, M. Hennemann, J.S. Murray, P. Politzer, Halogen bonding: the  $\sigma$ -hole, *J. Mol. Model.* 13 (2007) 291–296.
- [41] P. Politzer, J.S. Murray, T. Clark, Halogen bonding and other  $\sigma$ -hole interactions: a perspective, *Phys. Chem. Chem. Phys.* 15 (2013) 11178–11189.
- [42] A. Bondi, van der Waals volumes and radii, *J. Phys. Chem.* 68 (1964) 441–451.
- [43] M.E. Brezgunova, J. Lieffrig, E. Aubert, S. Dahaoui, P. Fertey, S. Lebègue, J.G. Ángyán, M. Fournigüé, E. Espinosa, Chalcogen bonding: experimental and theoretical determinations from electron density analysis. Geometrical preferences driven by electrophilic-nucleophilic interactions, *Cryst. Growth Des.* 13 (2013) 3283–3289.
- [44] T. Brinck, J.H. Stenlid, The molecular surface property approach: a guide to chemical interactions in chemistry, medicine, and material science, *Adv. Theory Simul.* 2 (2019) 1800149.
- [45] H. Wang, W. Wang, W.J. Jin,  $\sigma$ -Hole bond vs  $\pi$ -hole bond: a comparison based on halogen bond, *Chem. Rev.* 116 (2016) 5072–5104.
- [46] J. Andrés, P.W. Ayers, R.A. Boto, R. Carbó-Dorca, H. Chermette, J. Cioslowski, J. Contreras-García, D.L. Cooper, G. Frenking, C. Gatti, F. Heidar-Zadeh, L. Joubert, A. Martín Pendás, E. Matito, I. Mayer, A.J. Misquitta, Y. Mo, J. Pilmé, P.L.A. Popelier, M. Rahm, E. Ramos-Cordoba, P. Salvador, W.H. Eugen Schwarz, S. Shahbazian, B. Silvi, M. Solà, K. Szalewicz, V. Tognetti, F. Weinhold, É.-L. Zins, Nine questions on energy decomposition analysis, *J. Comput. Chem.* 40 (2019) 2248–2283.
- [47] T. Clark, Halogen bonds and  $\sigma$ -holes, *Faraday Discuss.* 203 (2017) 9–27.
- [48] P. Metrangolo, Y. Carcenac, M. Lahtinen, T. Pilati, K. Rissanen, A. Vij, G. Resnati, Nonporous organic solids capable of dynamically resolving mixtures of diiodoperfluoroalkanes, *Science* 323 (2009) 1461–1464.
- [49] C. Li, L. Li, X. Yang, W.J. Jin, Halogen bonding-assisted adsorption of iodoperfluoroarenes on a strong anion exchanger and its potential application in solid-phase extraction, *Colloids Surf. A* 520 (2017) 497–504.
- [50] A. Ballesteros-Gómez, L. Lunar, M.D. Sicilia, S. Rubio, Hyphenating supramolecular solvents and liquid chromatography: tips for efficient extraction and reliable determination of organics, *Chromatographia* 82 (2019) 111–124.
- [51] A.B. Lara, C. Caballo, M.D. Sicilia, S. Rubio, Speeding up the extraction of hexabromocyclododecane enantiomers in soils and sediments based on halogen bonding, *Anal. Chim. Acta* 1027 (2018) 47–56.
- [52] A.B. Lara, C. Caballo, M.D. Sicilia, S. Rubio, Enantiomer-specific determination of hexabromocyclododecane in fish by supramolecular solvent-based single-step sample treatment and liquid chromatography–tandem mass spectrometry, *Anal. Chim. Acta* 752 (2012) 62–68.
- [53] Q. Lv, S. Feng, L. Jing, Q. Zhang, M. Qi, J. Wang, H. Bai, R. Fu, Features of a truxene-based stationary phase in capillary gas chromatography for separation of some challenging isomers, *J. Chromatogr. A* 1454 (2016) 114–119.
- [54] Y. Yang, Z. Chang, X. Yang, M. Qi, J. Wang, Selectivity of hexaphenylbenzene-based hydrocarbon stationary phase with propeller-like conformation for aromatic and aliphatic isomers, *Anal. Chim. Acta* 1016 (2018) 69–77.
- [55] Y. Yang, Q. Wang, M. Qi, X. Huang,  $\pi$ -Extended triptycene-based material for capillary gas chromatographic separations, *Anal. Chim. Acta* 988 (2017) 121–129.
- [56] J. He, L. Yu, X. Huang, M. Qi, Triptycene-based stationary phases for gas chromatographic separations of positional isomers, *J. Chromatogr. A* 1599 (2019) 223–230.
- [57] Y. Zhang, Q. Lv, M. Qi, Z. Cai, Performance of permethyl pillar[5]arene stationary phase for high-resolution gas chromatography, *J. Chromatogr. A* 1496 (2017) 115–121.
- [58] P. Peluso, V. Mamane, E. Aubert, A. Dessì, R. Dallochio, A. Dore, P. Pale, S. Cossu, Insights into halogen bond-driven enantioseparations, *J. Chromatogr. A* 1467 (2016) 228–238.
- [59] A. Farina, S.V. Meille, M.T. Messina, P. Metrangolo, G. Resnati, G. Vecchio, Resolution of racemic 1,2-dibromohexafluoropropane through halogen-bonded supramolecular helices, *Angew. Chem. Int. Ed.* 38 (1999) 2433–2436.
- [60] M.T. Messina, P. Metrangolo, G. Resnati, Resolution of racemic perfluorocarbons through self-assembly driven by electron donor-acceptor intermolecular recognition, *ACS Symp. Ser.* 746 (2000) 239–254.
- [61] W.H. Pirkle, K.Z. Gan, L.J. Brice, The enhancement of enantioselectivity by halogen substituents, *Tetrahedron Asymmetry* 7 (1996) 2813–2816.
- [62] P. Peluso, V. Mamane, S. Cossu, Liquid chromatography enantioseparations of halogenated compounds on polysaccharide-based chiral stationary phases: role of halogen substituents in molecular recognition, *Chirality* 27 (2015) 667–684.
- [63] C. Gatti, F. Cargnoni, L. Bertini, Chemical information from the source function, *J. Comput. Chem.* 24 (2003) 422–436.
- [64] P. Peluso, A. Dessì, R. Dallochio, V. Mamane, S. Cossu, Recent studies of docking and molecular dynamics simulation for liquid-phase enantioseparations, *Electrophoresis* 40 (2019) 1881–1896.
- [65] J.A.V. Lopez, J.G. Petitbois, C.S. Vairappan, T. Umezawa, F. Matsuda, T. Okino, Columbamides D and E: chlorinated fatty acid amides from the marine cyanobacterium *Moorea bouillonii* collected in Malaysia, *Org. Lett.* 19 (2017) 4231–4234.
- [66] Z. He, F. Wu, W. Xia, L. Li, K. Hu, A.E. Kaziem, M. Wang, Separation and detection of cyproconazole enantiomers and its stereospecific recognition with chiral stationary phase by high-performance liquid chromatography, *Analyst* 144 (2019) 5193–5200.
- [67] R.K. Hofstetter, F. Potlitz, L. Schulig, S. Kim, M. Hasan, A. Link, Subcritical fluid chromatography at sub-ambient temperatures for the chiral resolution of ketamine metabolites with rapid-onset antidepressant effects, *Molecules* 24 (2019) 1927.
- [68] K. Eskandari, M. Lesani, Does fluorine participate in halogen bonding?, *Chem. Eur. J.* 21 (2015) 4739–4746.
- [69] D. Speybrouck, E. Lipka, Preparative supercritical fluid chromatography: a powerful tool for chiral separations, *J. Chromatogr. A* 1467 (2016) 33–55.
- [70] S. Khater, M.A. Lozac'h, I. Adam, E. Francotte, C. West, Comparison of liquid and supercritical fluid chromatography mobile phases for enantioselective separations on polysaccharide stationary phases, *J. Chromatogr. A* 1467 (2016) 463–472.
- [71] X. Zhu, Y. Lu, C. Peng, J. Hu, H. Liu, Y. Hu, Halogen bonding interactions between brominated ion pairs and CO<sub>2</sub> molecules: implications for design of new and efficient ionic liquids for CO<sub>2</sub> absorption, *J. Phys. Chem. B* 115 (2011) 3949–3958.
- [72] B. Chankvetadze, Recent development on polysaccharide-based chiral stationary phases for liquid-phase separation of enantiomers, *J. Chromatogr. A* 1269 (2012) 26–51.
- [73] Y. Okamoto, E. Yashima, Polysaccharide derivatives for chromatographic separation of enantiomers, *Angew. Chem. Int. Ed.* 37 (1998) 1020–1043.
- [74] Y. Okamoto, M. Kawashima, K. Hatada XI, Controlled chiral recognition of cellulose triphenylcarbamate derivatives supported on silica gel, *J. Chromatogr.* 363 (1986) 173–186.
- [75] E. Yashima, E. Kasashima, Y. Okamoto, Enantioseparation on 4-halogen-substituted phenylcarbamates of amylose as chiral stationary phases for high-performance liquid chromatography, *Chirality* 9 (1997) 63–68.
- [76] B. Chankvetadze, L. Chankvetadze, S. Sidamonidze, E. Kasashima, E. Yashima, Y. Okamoto, 3-Fluoro-, 3-chloro- and 3-bromo-5-methylphenylcarbamates of cellulose and amylose as chiral stationary phases for high-performance liquid chromatographic enantioseparation, *J. Chromatogr. A* 787 (1997) 67–77.
- [77] C. West, M.L. Konjaria, N. Shashvashvili, E. Lemasson, P. Bonnet, R. Kakava, A. Volonterio, B. Chankvetadze, Enantioseparation of novel chiral sulfoxides on chlorinated polysaccharide stationary phases in supercritical fluid chromatography, *J. Chromatogr. A* 1499 (2017) 174–182.
- [78] B. Zhu, Y. Yao, M. Deng, Z. Jiang, Q. Li, Enantioselective separation of twelve pairs of enantiomers on polysaccharide-based chiral stationary phases and thermodynamic analysis of separation mechanism, *Electrophoresis* 39 (2018) 2398–2405.
- [79] S. Terada, M. Hirai, A. Honzawa, O. Kitagawa, A. Kamizela, A. Wzorek, V.A. Soloshonok, Possible case of halogen bond-driven self-disproportionation of enantiomers (SDE) via achiral chromatography, *Chem. Eur. J.* 23 (2017) 14631–14638.
- [80] X.Q. Yan, X.R. Zhao, H. Wang, W.J. Jin, The competition of  $\sigma$ -hole...Cl<sup>-</sup> and  $\pi$ -hole...Cl<sup>-</sup> bonds between C<sub>6</sub>F<sub>5</sub>X (X = F, Cl, Br, I) and the chloride anion and its potential application in separation science, *J. Phys. Chem. B* 118 (2014) 1080–1087.